High-speed imaging in noncontact atomic force microscopy

M. Balantekin

Izmir Institute of Technology, Electrical & Electronics Engineering
Urla, Izmir 35430, Turkey mujdatbalantekin@iyte.edu.tr

ABSTRACT

We analyze the high-speed operating method that we recently developed to be used in noncontact atomic force microscopes (AFM). We simulated the method on various samples and it is shown that the method can minimize the time spent for noncontact AFM imaging experiments. The initial simulation results showed that even with an ordinary AFM cantilever imaging speeds faster than 10 frames/second can be achieved.

Keywords: atomic force microscope, high-speed AFM imaging, noncontact mode, eigenmode of a cantilever

1 INTRODUCTION

Atomic Force Microscope (AFM) has enabled high-resolution imaging, manipulation, and characterization of nanoscale structures, devices, and systems. Dynamic imaging modes of AFM provide better force sensitivity over contact mode. Hence the tapping and noncontact modes are the preferred operating modes in air and vacuum environments. However, imaging speeds of conventional noncontact AFM systems are not satisfactory for applications such as real-time imaging of biomolecular processes and industrial scale nanometrology. Moreover, it is important to minimize the error due to thermal and mechanical drift and the time spent for any nanoscale imaging experiment.

The past research on the high-speed AFM imaging has shown that two major factors that limit the scan speed are the bandwidth of the actuator and the transient response of the probe. The scanner, the electronic detector and the feedback controller have also effect on the scan speed [1–3]. To increase the imaging bandwidth, both the sensor and the actuator sizes must be minimized at the expense of increased system complexity [3–6]. In the recent studies, novel probes with integrated sensors and actuators were also designed [7-9]. Despite these efforts, the scan speeds required for the visualization of biomolecules have not been achieved with dynamic AFM systems.

2 METHOD

The dynamic AFM systems can be divided into two categories. The first one is the amplitude modulation (AM) AFM, or the tapping-mode, and the other one is the frequency modulation (FM) AFM, or the noncontact-mode [10]. The AM-AFM systems usually operated in air. The FM-AFM method was developed by Albrecht *et al.* [11] to increase the imaging bandwidth if the environment is a vacuum. The FM-AFM or the noncontact-mode AFM systems can be operated in air as well.

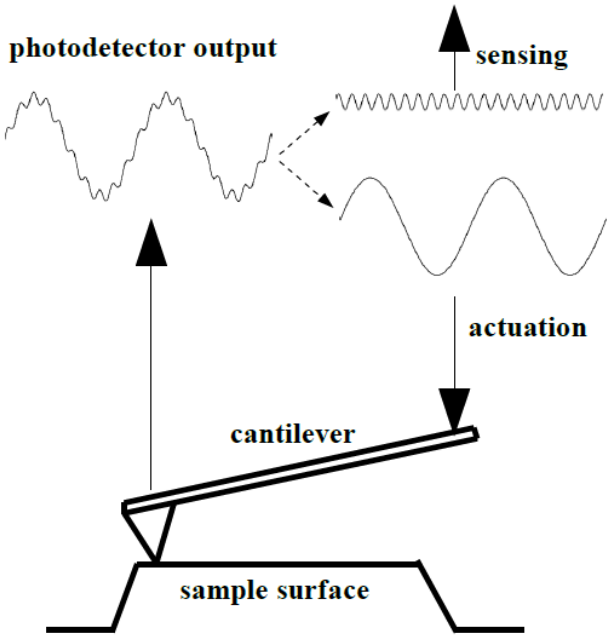

Figure 1: Description of the method.

Consider the tip-sampe system given in Fig. 1, where the cantilever is excited at both its fundamental and higher eigenmodes. Therefore the photodetector signal has two components. In the method that we proposed, the higher eigenmode oscillation is used for sensing and the fundamental eigenmode oscillation is used for actuation. We note that the amplitude of fundamental eigenmode oscillation is much larger than that of the higher eigenmode oscillation as seen in Fig. 1. The frequency of higher eigenmode oscillation depends on the tip-sample interaction force and any spontaneous change in the interaction force due to sample topography is detected by system electronics. The amplitude of the fundamental eigenmode is adjusted by the controller to keep the higher eigenmode oscillation frequency at a constant level.

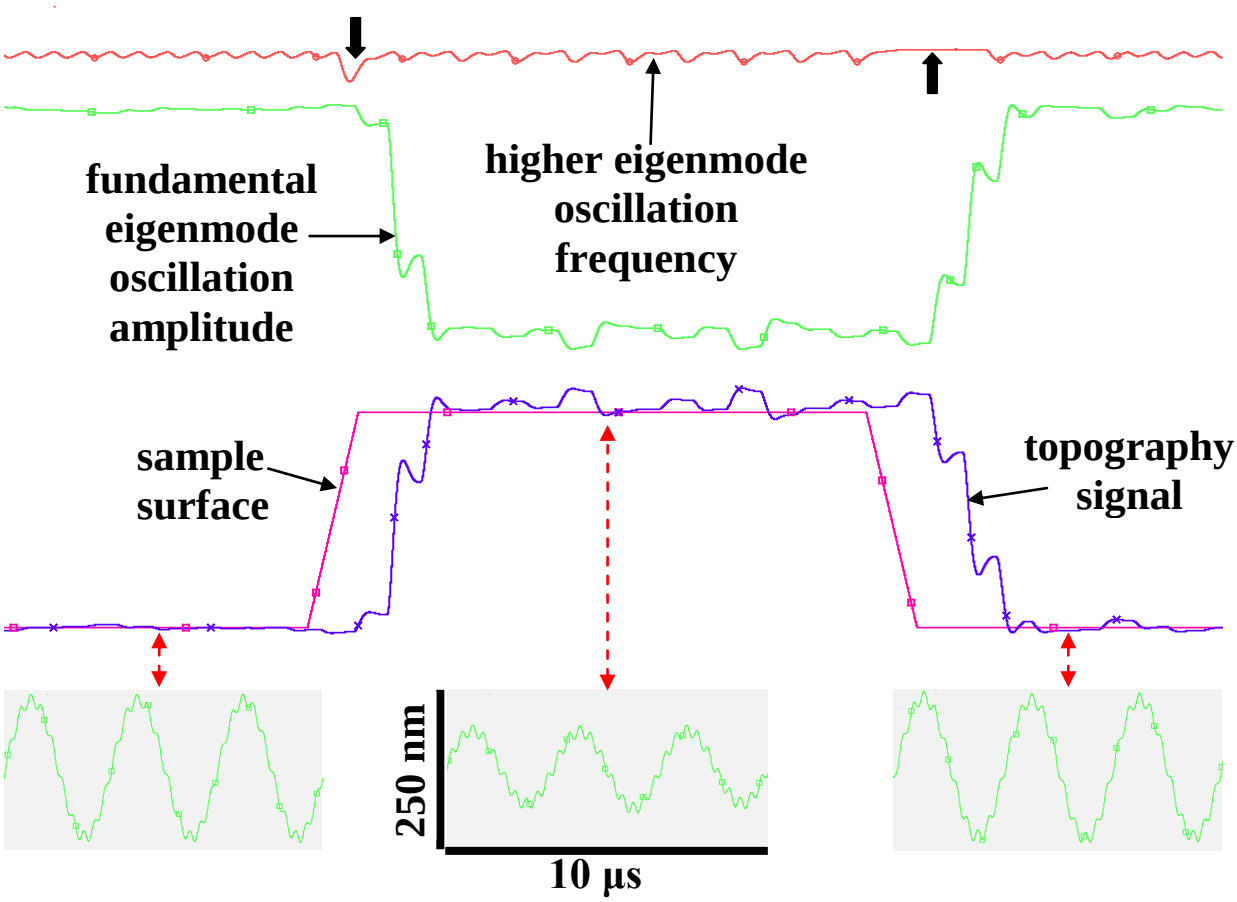

Figure 2: The obtained topography signal for the given 50 nm tall sample surface. Fundamental eigenmode oscillation amplitude and the higher eigenmode oscillation frequency signals are plotted in the same time interval. The total tip oscillation as a function of time is also shown at three different locations (indicated by dashed arrows).

In other words, the fundamental eigenmode oscillation amplitude is adjusted to perform the function of the actuator instead of a Z-piezo. The Z-piezo in conventional AFM systems is an important factor limiting the system bandwidth due to its low resonance frequency. On the other hand, an ordinary AFM cantilever can have a much higher resonance frequency. Therefore we expect a faster transient response with a cantilever. However, an AFM cantilever also has a high quality factor in air and vacuum environments. We solved this problem by applying the *Q*-control method [12–15] to reduce the artificial quality factor of the fundamental eigenmode. The method can be applied to the AM-AFM systems as well. A more elaborate description and the implementation of the method can be found elsewhere [16].

3 SIMULATION RESULTS

The proposed method is implemented and the time-domain simulations are performed in an electrical circuit simulator [17], where the mass, spring and damping constants of the cantilever are converted to the equivalent electrical elements and the attractive and repulsive interaction forces are realized using the controlled sources. We use the point-mass model for the fundamental and the higher eigenmodes. To model tip-sample interactions, we use Derjaguin-Muller-Toporov contact model of a spherical tip [18]. We also include the van der Waals forces to account for attractive surface forces.

The cantilever is kept oscillating at its higher-order resonant frequency via positive feedback with a free oscillation amplitude of 10 nm. The peak oscillation amplitude of the fundamental eigenmode is adjusted by the feedback controler that be changed from 50 nm to 200 nm, providing a 150 nm actuation range. In Fig. 2, we see a section from time-domain simulations. When the tip passes the rising (or falling) edge of the surface topography, the higher eigenmode frequency decreases (or increases), indicated by thick arrows. This variation in the higher eigenmode frequency controls the fundamental eigenmode amplitude. The decrease in the fundamental eigenmode oscillation amplitude basically moves the tip away from the sample and hence performs the function of an actuator.

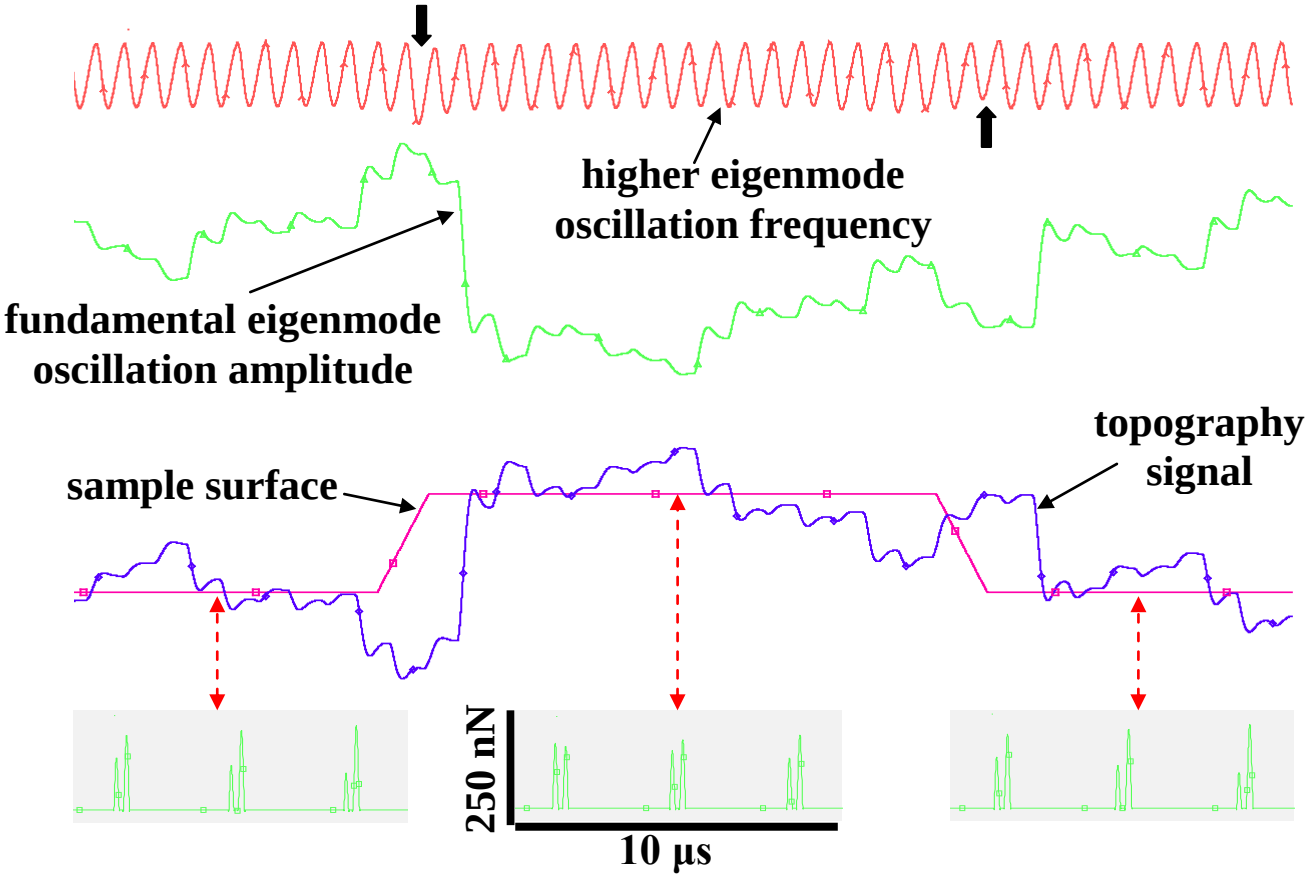

Figure 3: The obtained topography signal for the given 2 nm tall sample surface. Fundamental eigenmode oscillation amplitude and the higher eigenmode oscillation frequency signals are plotted in the same time interval. The tip-sample interaction force as a function of time is also shown at three different locations (indicated by dashed arrows).

The total tip oscillation as a function of time is plotted at three different locations showing how the actuation is done. By inverting the fundamental oscillation amplitude we can obtain the sample topography. The time interval for this simulation is approximately 150 μs, and the measurement error, defined in [19], is about 30%. Considering a sample that has 5 of these surface features in the fast scan axis, then the acquisition of 100 x 100 pixel image will take 150 μs x 5 x 100 = 75 ms. This means that imaging speed faster than 10 frames/sec is possible. Note that this result is obtained with an ordinary AFM cantilever that has a fundamental eigenmode resonance frequency of 300 kHz, stiffness of 10 N/m, and a quality factor of 100. The higher eigenmode has a resonance frequency of 3 MHz, stiffness of 100 N/m, and a quality factor of 100. The tip-sample parameters are also chosen to simulate a typical AFM experiment, where the tip radius is selected to be 10 nm and the effective tip-sample elasticity is 1 GPa.

We see that the fundamental eigenmode oscillation amplitude and hence the obtained topography is not smooth in the flat portions of the sample surface due to non-ideal characteristics of the detection electronics. We also performed simulation for a 2 nm tall sample surface. The result is seen in Fig. 3. The time interval for this simulation is again 150 μs, and the measurement error in this case is about 70%. Note that there is a ripple on the higher eigenmode oscillation frequency, but, it can still detect the edges of the sample surface (see thick arrows). In Fig. 3 we also plotted the peak transient forces at three different locations. The peak transient forces reach their maximum of about 250 nN due to an upward step in the surface topography. Unlike the traditional FM-AFM imaging where the tip oscillates mostly in the attractive force region, we selected the set-point such that the tip also enters the repulsive force region. We observe that the interaction force can have several repulsive peaks while the tip approaches the sample.

We also investigated the effect of sample stifness. We performed simulations on a 20 nm tall sample surface for 0.1 GPa and 10 GPa effective tip-sample elasticity. In these simulations, we use the same cantilever parameters and the same simulation time interval. The measurement error is

found to be less than 40% in both cases. The peak transient forces are less than 90 nN for 0.1 GPa sample and can be as high as 640 nN for 10 GPa sample.

4 CONCLUSION

High-speed imaging and characterization has become increasingly important. In this work, we briefly analyzed a new high-speed and dynamic AFM imaging method that we developed. We obtained the measurement error and peak transient forces for various samples. We found that the method can minimize the time spent for a noncontact AFM imaging experiments even with ordinary cantilevers. It may also enable the dynamic imaging systems to be used in applications such as real-time imaging of biomolecular processes and industrial scale nanometrology.

This work is supported by TUBITAK (Grant No. 110T732).

REFERENCES

[1] G. Schitter, P. Menold, H. F. Knapp, F. Allgower, and A. Stemmer, Rev. Sci. Instrum. 72, 3320 (2001).
[2] G. Schitter, F. Allgower, and A. Stemmer, Nanotechnology 15, 108 (2004).
[3] G. E. Fantner *et al.*, Ultramicroscopy 106, 881 (2006).
[4] M. B. Viani *et al.*, Rev. Sci. Instrum. 70, 4300 (1999).
[5] T. Ando, N. Kodera, E. Takai, D. Maruyama, K. Saito, and A. Toda, Proc. Natl. Acad. Sci. U.S.A. 98, 12468 (2001).
[6] T. Ando, T. Uchihashi, and T. Fukuma, Prog. Surf. Sci. 83, 337 (2008).
[7] F. L. Degertekin, A. G. Onaran, M. Balantekin, W. Lee, N. A. Hall, and C. F. Quate, Appl. Phys. Lett. 87, 213109 (2005).
[8] T. Sulchek *et al.*, Rev. Sci. Instrum. 71, 2097 (2000).
[9] T. Akiyama, U. Staufer, and N. F. de Rooij, Rev. Sci. Instrum. 73, 2643 (2002).
[10] R. Garcia and R. Perez, Surf. Sci. Rep. 47, 197 (2002).
[11] T. R. Albrecht, P. Grutter, D. Horne, and D. Rugar, J. Appl. Phys. 69, 668 (1991).
[12] J. Mertz, O. Marti, and J. Mlynek, Appl. Phys. Lett. 62, 2344 (1993).
[13] T. Sulchek *et al.*, Appl. Phys. Lett. 76, 1473 (2000).
[14] M. Antognozzi, M. D. Szczelkun, A. D. L. Humphris, and M. J. Miles, Appl. Phys. Lett. 82, 2761 (2003).
[15] N. Kodera, H. Yamashita, and T. Ando, Rev. Sci. Instrum. 76, 53708 (2005).
[16] M. Balantekin, (submitted to publication).
[17] M. Balantekin and A. Atalar, Appl. Surf. Sci. 205, 86 (2003).
[18] *Handbook of Micro/Nanotribology*, B. Bhushan (CRC, Boca Raton, Florida, 1999).
[19] M. Balantekin and F. L. Degertekin, Ultramicroscopy 111, 1388 (2011).